Laser Thermal Ablation: Model and Parameter Estimates to Predict Cell Death from MR Thermometry Images

M. S. Breen[1], K. Butts[2], L. Chen[3], G. M. Saidel[1], D. L. Wilson[1]

[1]Department of Biomedical Engineering, Case Western Reserve University, Cleveland, OH, United States, [2]Department of Radiology, Stanford University, Stanford, CA, United States, [3]Fox Chase Cancer Center, Philadelphia, PA, United States

Introduction

Solid tumors and other pathologies can be treated using laser thermal ablation under interventional magnetic resonance image (MRI) guidance. To monitor an ablation procedure, MRI can continuously acquire temperature images during heating, and structural images during and after heating. We are investigating the ability to monitor treatment using MR thermometry measurements. A model relating temperature history to cell death could be used to predict the therapeutic region in real-time during the heating process, thereby allowing one to treat the pathology and spare adjoining critical tissues.

Methods

We developed a model that predicts cell death based on the local time-varying temperature. At elevated temperatures, we assume that there will be destruction to tissue in a region starting in the native condition. The build up of destruction will depend both upon temperature (T) and duration through a temperature dependent rate coefficient, $\beta[T(t)]$. The accumulated destruction of tissue, $\Omega(t)$, at time, t, is defined by Equation 1. Above a critical temperature, T_C, the destruction of tissue can occur. Since the rate of tissue destruction is expected to increase with temperature, β is expected to be a monotonically increasing function with respect to temperature, as shown in Equation 2. The severity of the accumulated destruction increases to a critical threshold value, Ω_C, that leads to cell death. This critical threshold is based on an all or nothing tissue response observed in histology minutes post-ablation that shows a sharp transition between dead and adjacent normal cells [1].

$$\Omega(t) = 1 - \exp\left\{-\int_0^t \beta\left[T(\tau)\right] d\tau\right\} \qquad (1),$$

$$\beta[T(t)] = \begin{cases} 0, & T(t) < T_c \\ A\left[T(t) - T_c\right]^N, & T(t) \geq T_c \end{cases} \qquad (2).$$

To correlate the model predicted regions of cell death with the tissue response, we created a thermal lesion in seven in vivo rabbit brains. We used a clinical 0.5 T MR imaging system with an extremity coil to guide a laser fiber into each brain, and continuously acquire gradient-echo (GE) MR images (TR = 77.2 msec; TE = 38.9 msec; flip angle = 30°; 256 x 128 matrix; 16 x 16 cm field of view (FOV); one 3.0 mm thick section, 10 sec acq. time) before, during, and after heating. At four hours post-ablation, we acquired T2-weighted spin-echo MR images (TR = 4000 msec; TE = 115 msec; 512 x 256 matrix; 16 x 16 cm FOV; one 2.0 mm thick section) in the same orientation as the GE MR images. Lesion formation was achieved with an Nd:YAG laser. Heating durations varied between 30 and 581 sec. To process the temperature maps from the GE MR images, we subtracted pre-ablation baseline phase maps from remaining phase maps. We used a proton resonance frequency thermal coefficient of 0.01 ppm/°C. We removed noise in the temperature maps with a temporal filter. To compare model predicted regions of cell death with the tissue response, we aligned the post-ablation MR image to the GE MR images used for temperature maps with a rigid-body registration that aligned fiducials near the lesion.

Results

In Figure 1, the post-ablation T2-weighted MR lesion images show a distinct circular hyperintense rim surrounding a central hypointense core. It was previously shown that the outer boundary of the hyperintense rim corresponds to the boundary of cell death as seen in registered histology images on the order of one MR voxel (0.70 mm) [1]. We manually segmented the boundary of cell death in the registered post-ablation MR image, and created a binary image of the cell death region to compare with the modeled tissue damage region on a voxel-by-voxel basis. Model parameters were simultaneously estimated with an iterative optimization using every interesting voxel (4375 voxels) in 328 temperature images from the seven experiments. In Figure 2, we plotted as a function of lesion, the number of false positives (FP) and false negatives (FN). The number of FP and FN were small as compared to the size of the actual cell death region. For a necrotic region of 766 voxels across all lesions, the model provided a voxel specificity and sensitivity of 98.1% and 78.5%, respectively. Mislabeled voxels were typically within one voxel from the segmented necrotic boundary with median distances of 0.77 mm and 0.22 mm for FP and FN, respectively. We compared our model to the critical temperature model that assumes cell death is not observable below a critical temperature and occurs rapidly and completely above the critical temperature [2]. Across all lesions, our model predicted 13 fewer FP voxels (1.8 million cells) and 57 fewer FN voxels (8.2 million cells), with the number of cells in a voxel based on a cubic cell with a 20 μm edge length.

Discussion

We can compare our model and data analysis technique to previously reported ones. Arrhenius-based models with parameters from other experiments not surprisingly did not always work [2]. A critical temperature model typically performed better [2-3]. However, this model neglects the heating duration and is sensitive to transient noise in the temperature data. We use a model that considers the temperature history, and had fewer errors than the critical temperature model. This model in principal will be able to predict cell death for a wider range of temperature histories. Our analysis method uses all interesting voxels unlike previous reports which only analyzed voxels along the segmented cell death boundary [2-4]. Hence, in theory, we can more precisely assess the model fit error.

We conclude that our model coupled with a sequence of MR temperature maps can be used to accurately predict the tissue response. Features such as accurate image registration, filtering, and parameter optimization are important steps to accurately fit the model to the segmented region of cell death. Results show that for rabbit brain, the estimated region of necrosis closely corresponds to the actual cell death region. This is good evidence that our model can predict the therapeutic region.

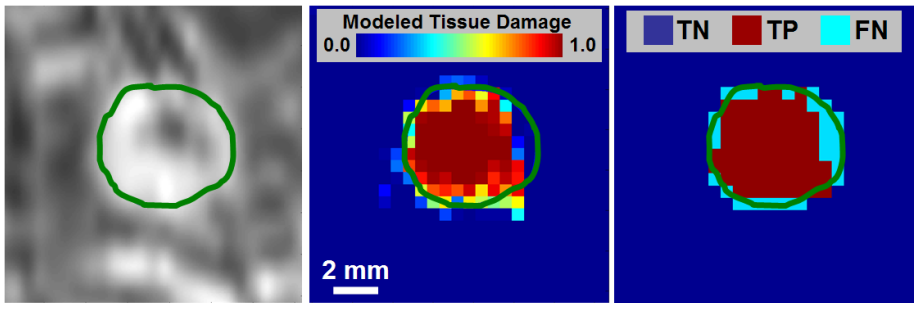

Figure 1: Comparison of segmented cell death boundary (green) with modeled tissue damage map (middle) and difference map (right) of the model fit error for a typical lesion. The cell death boundary was manually segmented in the registered T2-weighted MR lesion image (left) and copied to the color-coded modeled tissue damage and difference maps. In the difference map, each voxel was color-coded as either true negative (TN), true positive (TP), or false negative (FN). For this lesion (lesion 3), only voxels along the boundary of the cell death region were mislabeled as FN, with no false positive (FP) voxels.

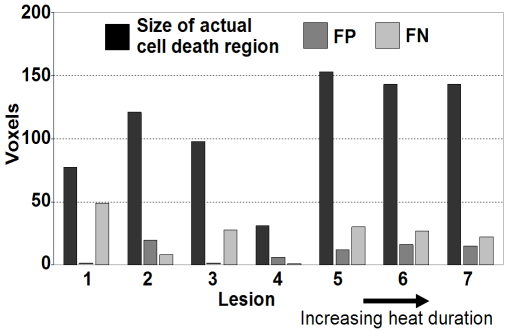

Figure 2: Plotted are the lesion size, number of false positives (FP), and number of false negatives (FN) for each thermal lesion. The FP and FN voxels correspond to the model's overestimation and underestimation of the actual cell death region, respectively. For lesion 1 and 3, there were no FP.

References

[1] Breen MS, et. al., J Magn Reson Imaging, 2004; 20:475-486.
[2] Chen L, et. al., J Magn Reson Imaging, 2002; 16:147-152.
[3] Peters RD, et. al., Magn Reson Med, 2000; 44:873-883.
[4] Graham SJ, et. al., Magn Reson Med, 1999; 41:321-328.